Int. J. Heat Mass Transfer. Vol. 33, No. 3, pp. 417–425, 1990
Printed in Great Britain

0017–9310/90 $3.00 + 0.00

Laminar-flow heat transfer to a fluid flowing axially between cylinders with a uniform surface temperature

O. MIYATAKE
Department of Chemical Engineering, Kyushu University, Fukuoka 812, Japan

and

H. IWASHITA
Thermal-Energy System Engineering, Graduate School, Kyushu University, Kasuga 816, Japan

(*Received* 7 *March* 1989 *and in final form* 17 *May* 1989)

Abstract—This paper deals with the laminar-flow heat transfer to a fluid flowing axially between a triangular or a square array of cylinders with a uniform wall temperature. The energy equation in finite-difference form is solved to obtain the axial variation of the cross-sectional temperature distribution, and the numerical results for the local Nusselt number Nu_{loc} and the logarithmic-mean Nusselt number Nu_{lm} are presented. From the results, correlating equations suitable for predicting Nu_{loc} and Nu_{lm} are derived as functions of the pitch-to-diameter ratio σ and the local Graetz number Gz_{loc} or the Graetz number Gz. It is found that, at the same volume fractions of cylinders ε, the heat transfer coefficient for the triangular array is larger than that for the square array, especially for the case $\varepsilon > 0.5$.

1. INTRODUCTION

MOST OF the research that has been carried out on heat transfer to a fluid flowing axially between cylinders has been concerned with turbulent-flow heat transfer in relation to the cooling of the fuel rods in a nuclear reactor [1, 2]. The only research done on laminar-flow heat transfer has dealt with an axially uniform heat flux on the wall of the cylinders in a triangular array or a square array. Apart from analytical [3, 4] and numerical [5–7] results for the asymptotic local Nusselt number when the axial distance becomes large, little is known about the characteristics of axially varying heat transfer in this geometry.

A knowledge of the heat transfer characteristics of laminar flow in the axial direction is required for the design of multi-tubular heat exchangers for highly viscous liquids, the analysis of heat transfer in geometrically similar systems, and the analysis of rod-bank regenerators [8].

This paper reports on a numerical study on the characteristics of axially varying heat transfer to a fluid flowing axially between cylinders, which are arranged in a triangular or a square array, with a uniform peripheral and axial wall temperature.

2. MATHEMATICAL FORMULATION

The analytical system and coordinates are shown in Fig. 1. A cylindrical coordinate system (r, θ, z) in the radial, circumferential, and axial directions was used for the analysis of heat transfer to a fluid flowing with laminar flow in the axial direction between a triangular or a square array of cylinders of diameter d_o, radius r_o, length l, and spaced $2s$ apart. From the symmetry of the cross-section of flow area, the element to be analyzed is a right-angled triangular prism of base s, $\pi/6$ for a triangular array or $\pi/4$ for a square array, and length l.

The following assumptions are made: (1) the wall of each cylinder in the heat transfer region ($z \geqslant 0$) is at a uniform peripheral and axial temperature t_w; (2) the fluid enters the heat transfer region at a uniform temperature t_0 and flows through the heat transfer region with a fully developed laminar velocity distribution; (3) the physical properties of the fluid are constant, and viscous dissipation can be ignored; and (4) axial heat conduction through the fluid is negligible in comparison with the convective transfer.

On this basis, the energy equation and the boundary conditions of temperature are

$$v\frac{\partial t}{\partial z} = \alpha\left\{\frac{1}{r}\frac{\partial}{\partial r}\left(r\frac{\partial t}{\partial r}\right) + \frac{1}{r^2}\frac{\partial^2 t}{\partial \theta^2}\right\} \tag{1}$$

$$z = 0; \quad t = t_0 \tag{2}$$

$$r = r_o; \quad t = t_w \tag{3}$$

$$r = r^+ = \frac{s}{\cos\theta}; \quad \frac{\partial t}{\partial n} = \frac{\partial t}{\partial r}\cos\theta - \frac{\partial t}{\partial \theta}\frac{\sin\theta}{r} = 0 \tag{4}$$

$$\theta = 0, \quad \theta = \theta^+; \quad \partial t/\partial\theta = 0 \tag{5}$$

where

NOMENCLATURE

A dimensionless flow area per cylinder (equation (14))
c_p heat capacity of fluid at constant pressure [J kg^{-1} K^{-1}]
d_o diameter of cylinder [m]
F, f, g functions of σ (equations (14), (37) and (39), respectively)
Gz Graetz number, wc_p/kl
Gz_{loc} local Graetz number, wc_p/kz
h_{lm} logarithmic-mean heat transfer coefficient (equation (16)) [W m^{-2} K^{-1}]
h_{loc} local heat transfer coefficient (equation (15)) [W m^{-2} K^{-1}]
K number of nodal points in angular direction
k thermal conductivity of fluid [W m^{-1} K^{-1}]
L dimensionless length of cylinder, $l\alpha/r_o^2 v_m$
l length of cylinder [m]
Nu_{lm} logarithmic-mean Nusselt number, $h_{lm}d_o/k$
Nu_{loc} local Nusselt number, $h_{loc}d_o/k$
n normal coordinate [m]
q_w heat flux at wall [W m^{-2}]
R dimensionless radial coordinate, r/r_o
r radial coordinate [m]
r_o radius of cylinder [m]
s half pitch between cylinders [m]
T dimensionless temperature, $(t-t_0)/(t_w-t_0)$
t temperature [K]
V dimensionless axial velocity, v/v_m
v axial velocity of fluid [m s^{-1}]
v_m mean axial velocity [m s^{-1}]
w mass flow rate of fluid per cylinder [kg s^{-1}]
Z dimensionless axial coordinate, $z\alpha/r_o^2 v_m$
z axial coordinate [m].

Greek symbols
α thermal diffusivity of fluid [m^2 s^{-1}]
Δ_j, δ_j constants
ε volume fraction of cylinders (equation (32))
θ angular coordinate [rad]
ρ density of fluid [kg m^{-3}]
σ pitch-to-diameter ratio, s/r_o $(= 2s/d_o)$
ϕ dimensionless spacing between cylinders, $\sigma - 1$.

Superscript
$\bar{x}$ peripherally averaged, $\int_0^{\theta^+} x\, d\theta/\theta^+$.

Subscripts
b fluid bulk mean
w cylinder wall
0 inlet, asymptote for small z or l
∞ asymptote for large z or l.

Abbreviations
[SA] square array
[TA] triangular array.

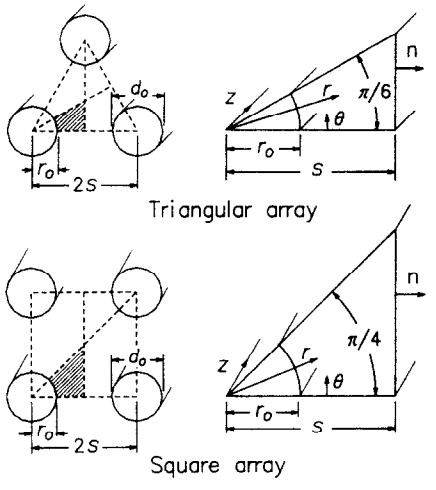

FIG. 1. Analytical system and coordinates.

$$\theta^+ = \frac{\pi}{6}\text{[TA]}, \quad \theta^+ = \frac{\pi}{4}\text{[SA]} \tag{6}$$

[TA] and [SA] represent a triangular array and a square array of cylinders, respectively.

The dimensionless quantities

$$V = \frac{v}{v_m}, \quad T = \frac{t-t_0}{t_w-t_0}, \quad R = \frac{r}{r_o},$$
$$Z = \frac{z\alpha}{r_o^2 v_m}, \quad \sigma = \frac{s}{r_o} \tag{7}$$

are introduced, so as to put equations (1)–(5) into dimensionless form

$$V\frac{\partial T}{\partial Z} = \frac{1}{R}\frac{\partial}{\partial R}\left(R\frac{\partial T}{\partial R}\right) + \frac{1}{R^2}\frac{\partial^2 T}{\partial \theta^2} \tag{8}$$

$$Z = 0; \quad T = 0 \tag{9}$$

$$R = 1; \quad T = 1 \tag{10}$$

$$R = R^+ = \frac{\sigma}{\cos\theta}; \quad \frac{\partial T}{\partial R}\cos\theta - \frac{\partial T}{\partial \theta}\frac{\sin\theta}{R} = 0 \tag{11}$$

$$\theta = 0, \quad \theta = \theta^+; \quad \partial T/\partial\theta = 0. \tag{12}$$

The dimensionless velocity V is given by the following analytical expressions [9]:

Table 1. Values of $\Delta_j \times 10^2$

j	$\sigma = 1.0$	$\sigma = 1.001$	$\sigma = 1.01$	$\sigma = 1.02$	$\sigma = 1.05$	$\sigma = 1.1$	$\sigma = 1.2$
1	−3.05502	−3.06870	−3.19004	−3.32065	−3.68059	−4.15694	−4.69398
2	0.53311	0.53247	0.52368	0.50801	0.43358	0.28029	0.06781
3	−0.03019	−0.02841	−0.01295	0.00239	0.03169	0.03782	0.01749
4	−0.01697	−0.01702	−0.01651	−0.01440	−0.00568	0.00108	0.00131
5	0.00135	0.00113	−0.00051	−0.00157	−0.00152	−0.00024	0.00006
6	0.00128	0.00125	0.00084	0.00035	−0.00017	−0.00005	0.00000
7	0.00013	0.00015	0.00024	0.00018	−0.00000	−0.00001	
8	−0.00009	−0.00008	0.00001	0.00004		−0.00000	
9	−0.00005	−0.00004	−0.00002	0.00000			
10	−0.00001	−0.00001	−0.00001				

j	$\sigma = 1.5$	$\sigma = 2.0$	$\sigma = 4.0$	$\sigma = \infty$	$\varepsilon = 0.75$	$\varepsilon = 0.50$	$\varepsilon = 0.25$
1	−5.02447	−5.04988	−5.05072	−5.05072	−4.15404	−4.95636	−5.04921
2	−0.06992	−0.08054	−0.08089	−0.08089	0.28135	−0.04145	−0.08026
3	0.00014	−0.00122	−0.00126	−0.00126	0.03787	0.00377	−0.00118
4	0.00008	−0.00002	−0.00002	−0.00002	0.00106	0.00035	−0.00001
5	0.00001	−0.00000	−0.00000	−0.00000	−0.00025	0.00002	0.00000
6	0.00000				−0.00005	0.00000	
7					−0.00001		

$$V = \frac{\sigma^2 A}{F}\left\{\frac{\sqrt{3}}{\pi}\ln R - \frac{R^2-1}{4\sigma^2} + \sum_{j=1}^{\infty}\frac{\Delta_j \cos 6j\theta}{6j\sigma^{6j}}\left(R^{6j} - \frac{1}{R^{6j}}\right)\right\} \quad \text{[TA]}$$

$$V = \frac{\sigma^2 A}{F}\left\{\frac{2}{\pi}\ln R - \frac{R^2-1}{4\sigma^2} + \sum_{j=1}^{\infty}\frac{\delta_j \cos 4j\theta}{4j\sigma^{4j}}\left(R^{4j} - \frac{1}{R^{4j}}\right)\right\} \quad \text{[SA]} \quad (13)$$

where

$$A = 2\sqrt{3}\sigma^2 - \pi \ \text{[TA]}, \quad A = 4\sigma^2 - \pi \ \text{[SA]} \quad (14)$$

$$F = \sigma^4\left\{\frac{6}{\pi}\left(\ln\frac{2\sqrt{3}\sigma}{3} - \frac{3}{2}\right) + \frac{13\sqrt{3}}{18} + \sum_{j=1}^{\infty}\frac{\Delta_j}{j}\left(\frac{1}{3j+1}\int_0^{\theta^+}\frac{\cos 6j\theta}{(\cos\theta)^{6j+2}}\,d\theta + \frac{1}{\sigma^{12j}(3j-1)}\int_0^{\theta^+}\frac{\cos 6j\theta}{(\cos\theta)^{2-6j}}\,d\theta\right)\right\} + \sqrt{3}\sigma^2 - \frac{\pi}{8} \quad \text{[TA]}$$

$$F = \sigma^4\left\{\frac{4}{\pi}(\ln 2\sigma^2 - 3) + \frac{4}{3} + \sum_{j=1}^{\infty}\frac{\delta_j}{j}\left(\frac{1}{2j+1}\int_0^{\theta^+}\frac{\cos 4j\theta}{(\cos\theta)^{4j+2}}\,d\theta + \frac{1}{\sigma^{8j}(2j-1)}\int_0^{\theta^+}\frac{\cos 4j\theta}{(\cos\theta)^{2-4j}}\,d\theta\right)\right\} + 2\sigma^2 - \frac{\pi}{8} \quad \text{[SA]} \quad (15)$$

and Δ_j and δ_j are constants, the recalculated and replenished values of which are listed in Tables 1 and 2, respectively, for σ and ε (see equation (32)) treated in the present numerical analysis.

The local heat transfer coefficient h_{loc}, which is based on the peripherally averaged wall heat flux $\overline{q_w}$ and the wall-to-bulk temperature difference $(t_w - t_b)$, is given by

$$h_{\text{loc}}(t_w - t_b)_{z=z} = -k\overline{(\partial t/\partial r)_w} = \overline{q_w}. \quad (16)$$

Taking a heat balance between $z = 0$ and l, the logarithmic-mean heat transfer coefficient h_{lm} is given by

$$h_{\text{lm}}\pi d_o l \Delta t_{\text{lm}} = wc_p(t_b - t_0)_{z=l} \quad (17)$$

where Δt_{lm} is the logarithmic-mean temperature difference

$$\Delta t_{\text{lm}} = \frac{(t_w - t_0) - (t_w - t_b)_{z=l}}{\ln\{(t_w - t_0)/(t_w - t_b)_{z=l}\}} \quad (18)$$

and w is the mass flow rate of fluid per cylinder given by

$$w = v_m \rho r_o^2 A. \quad (19)$$

The local Nusselt number Nu_{loc} and the logarithmic-mean Nusselt number Nu_{lm} are obtained from the dimensionless forms of equations (16)–(19)

$$Nu_{\text{loc}} = \frac{h_{\text{loc}} d_o}{k} = -\frac{2\overline{(\partial T/\partial R)_w}}{(1 - T_b)_{Z=Z}} \quad (20)$$

$$Nu_{\text{lm}} = \frac{h_{\text{lm}} d_o}{k} = -\frac{A}{\pi L}\ln(1 - T_b)_{Z=L} \quad (21)$$

where

$$L = l\alpha/r_o^2 v_m \quad (22)$$

Table 2. Values of $\delta_j \times 10^2$

j	$\sigma = 1.0$	$\sigma = 1.001$	$\sigma = 1.01$	$\sigma = 1.02$	$\sigma = 1.05$	$\sigma = 1.1$	$\sigma = 1.2$
1	−8.03471	−8.05613	−8.24661	−8.45302	−9.03578	−9.87211	−11.04208
2	1.03832	1.03348	0.98719	0.92996	0.73105	0.36595	−0.23868
3	0.24491	0.24778	0.27090	0.29151	0.32105	0.29108	0.15663
4	−0.05010	−0.04856	−0.03418	−0.01832	0.02065	0.04653	0.03500
5	−0.03008	−0.03003	−0.02871	−0.02552	−0.01197	0.00243	0.00532
6	−0.00376	−0.00407	−0.00622	−0.00740	−0.00579	−0.00114	0.00064
7	0.00243	0.00226	0.00076	−0.00052	−0.00158	−0.00053	0.00006
8	0.00172	0.00168	0.00122	0.00061	−0.00028	−0.00016	0.00000
9	0.00051	0.00053	0.00057	0.00041	−0.00001	−0.00004	
10	−0.00002	0.00001	0.00015	0.00016	0.00002	−0.00001	

j	$\sigma = 1.5$	$\sigma = 2.0$	$\sigma = 4.0$	$\sigma = \infty$	$\varepsilon = 0.75$	$\varepsilon = 0.50$	$\varepsilon = 0.25$
1	−12.25973	−12.50984	−12.53816	−12.53827	−8.52040	−11.44273	−12.46381
2	−0.90598	−1.04281	−1.05826	−1.05832	0.90971	−0.45710	−1.01768
3	−0.02081	−0.05713	−0.06120	−0.06122	0.29715	0.09939	−0.05049
4	0.00333	−0.00318	−0.00390	−0.00390	−0.01323	0.02519	−0.00200
5	0.00081	−0.00014	−0.00024	−0.00024	−0.02417	0.00407	0.00003
6	0.00012	−0.00000	−0.00002	−0.00002	−0.00752	0.00054	0.00002
7	0.00001		−0.00000	−0.00000	−0.00084	0.00006	0.00000
8	0.00000				0.00044	0.00001	
9					0.00035	0.00000	
10					0.00015		

$$T_b = \int_0^{\theta^+}\int_1^{R^-} TVR\,dR\,d\theta \Big/ \int_0^{\theta^+}\int_1^{R^-} VR\,dR\,d\theta. \tag{23}$$

By defining the local Graetz number Gz_{loc} and the Graetz number Gz as

$$Gz_{loc} = wc_p/kz = A/Z \tag{24}$$

$$Gz = wc_p/kl = A/L \tag{25}$$

Nu_{loc} becomes a function of σ and Gz_{loc}, and Nu_{lm} becomes a function of σ and Gz.

3. THE ASYMPTOTIC NUSSELT NUMBER

In the high Graetz number region ($z, l \to 0$), the asymptotic solution of Leveque [10], obtained by assuming that the velocity distribution in the thin temperature boundary layer is linear with a slope equal to the velocity gradient at the wall, can be extended to give the following expression for the peripherally averaged wall heat flux $\overline{q_w}$:

$$\overline{q_w} = \frac{k(t_w - t_0)}{\Gamma(4/3)} \frac{\overline{(\partial v/\partial r)_w^{1/3}}}{(9\alpha z)^{1/3}}. \tag{26}$$

As $t_b \approx t_0$ in this region, the asymptotic local heat transfer coefficient $h_{loc,0}$ is related to $\overline{q_w}$ as

$$h_{loc,0}(t_w - t_0) = \overline{q_w} \tag{27}$$

and, similarly, the asymptotic logarithmic-mean heat transfer coefficient $h_{lm,0}$ as

$$h_{lm,0}(t_w - t_0) = \frac{1}{l}\int_0^l \overline{q_w}\,dz. \tag{28}$$

Equating equations (26) and (27), and putting the result into dimensionless form, gives the following expression for the asymptotic local Nusselt number $Nu_{loc,0}$ in this region:

$$Nu_{loc,0} = \frac{2}{\Gamma(4/3)} \frac{\overline{(\partial V/\partial R)_w^{1/3}}}{(9A)^{1/3}} Gz_{loc}^{1/3}. \tag{29}$$

Similarly, substituting equation (26) into equation (28), integrating from $z = 0$ to l, and putting the result into dimensionless form, gives for the asymptotic logarithmic-mean Nusselt number $Nu_{lm,0}$ in this region

$$Nu_{lm,0} = (3/2)(Nu_{loc,0})_{Z=L}. \tag{30}$$

On the other hand, in the low Graetz number region ($z, l \to \infty$), the asymptotic local Nusselt number $Nu_{loc,\infty}$ and the asymptotic logarithmic-mean Nusselt number $Nu_{lm,\infty}$ are numerically equal. Therefore

$$Nu_{loc,\infty} = Nu_{lm,\infty}. \tag{31}$$

4. METHOD OF NUMERICAL ANALYSIS

The analysis was performed first by writing the energy equation in finite-difference form, and then solving it by the forward-marching, implicit method with iteration at each level of Z. The detailed procedure can be found in refs. [11, 12].

The number of equally spaced finite-difference nodal points in the θ-direction over the range $\theta = 0 - \theta^+$ was K; in the R-direction about $K(1+3.7\cos^{-1}\sqrt{(1/\sigma)})$ [TA] or $K(1+2.5\cos^{-1}\sqrt{(1/\sigma)})$ [SA] unequally spaced nodal points were used over the range $R = 1 - \sigma/\cos\theta^+$, and in the Z-direction 50 unequally spaced nodal points were set, each time Z increased by an order of magnitude, that is, the value of Z increased tenfold.

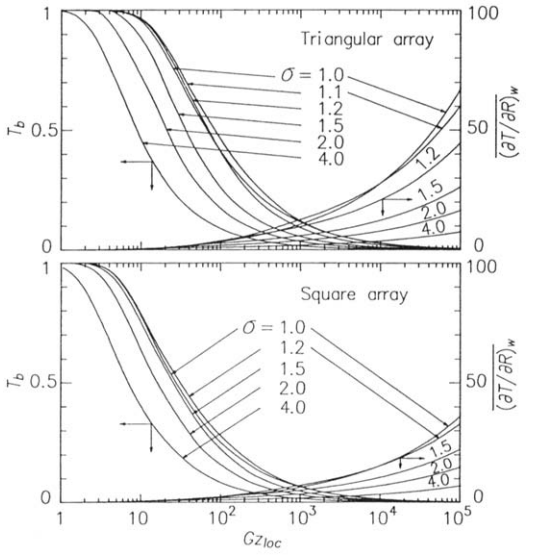

FIG. 2. Variation of dimensionless bulk temperature and dimensionless temperature gradient at wall with local Graetz number.

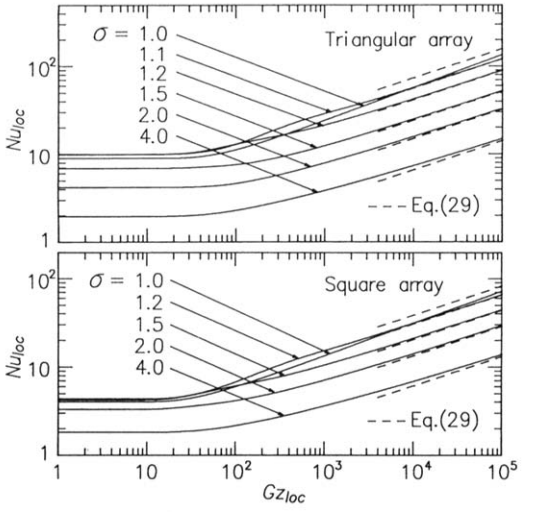

FIG. 3. Variation of local Nusselt number with local Graetz number.

$K = 41$ and 61 for $\sigma = 1.0$–1.1, $K = 21$ and 31 for $\sigma = 1.2$–2.0, and $K = 11$ and 21 for $\sigma = 4.0$ [TA] or $K = 46$ and 61 for $\sigma = 1.0$–1.02, and $K = 31$ and 46 for $\sigma = 1.05$–4.0 [SA].

In the finite-difference approximation of the energy equation, the central-difference approximation was used in the R- and θ-directions, and in the Z-direction the backward-difference approximation, in which the accuracy was improved by using three levels of Z, i.e. the calculating level and the nearest two upstream levels of Z. A quadratic curve was used for the finite-difference approximation of the temperature gradient at the boundaries.

The first step was to calculate V at each nodal point for the given value of σ, then to set the boundary condition for $Z = 0$, and to begin the calculation at a very low value of Z corresponding to a local Graetz number greater than 5×10^6. The iterative calculation for each level of Z was terminated when the absolute values of the differences between the values of T at all the nodal points in the R- and θ-directions before and after the iteration were below 10^{-8}. The calculations then advanced to a higher level of Z.

5. RESULTS OF NUMERICAL ANALYSIS

Figure 2 shows the variation of the dimensionless bulk temperature T_b and the peripherally averaged dimensionless temperature gradient at the wall $\overline{(\partial T/\partial R)_w}$ with Gz_{loc}, with the pitch-to-diameter ratio σ as a parameter. As a matter of course, T_b and $\overline{(\partial T/\partial R)_w}$ approach 1 and 0, respectively, for small Gz_{loc}. The value of T_b, that is, the heat transfer rate first increases and then slightly decreases as σ is reduced. The reason for this behavior is that, as σ is reduced, the decrease in the flow area increases the velocity gradient at the wall and thereby increases the heat transfer rate; below a certain value of σ, however, the velocity gradient at the wall at $\theta \approx 0$ decreases and this decreases the heat transfer rate.

Figures 3 and 4 show the variation of Nu_{loc} and Nu_{lm} with Gz_{loc} and Gz, respectively, with σ as a parameter. These figures reveal that Nu_{loc} and Nu_{lm} increase and then slightly decrease, as σ is reduced (see also Fig. 8 for small σ). The broken lines in Figs. 3 and 4 represent equations (29) and (30), respectively. Nu_{loc} and Nu_{lm} tend to approach equations (29) and (30), respectively, for large Gz_{loc} and Gz.

Figure 5 shows the variation of $Nu_{loc,\infty}$ $(= Nu_{lm,\infty})$ with the dimensionless spacing between cylinders ϕ $(= \sigma - 1)$. Ⓣ represents the present numerical solu-

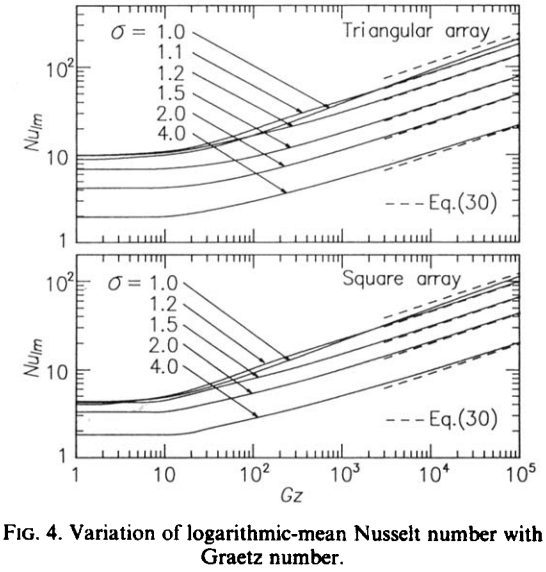

FIG. 4. Variation of logarithmic-mean Nusselt number with Graetz number.

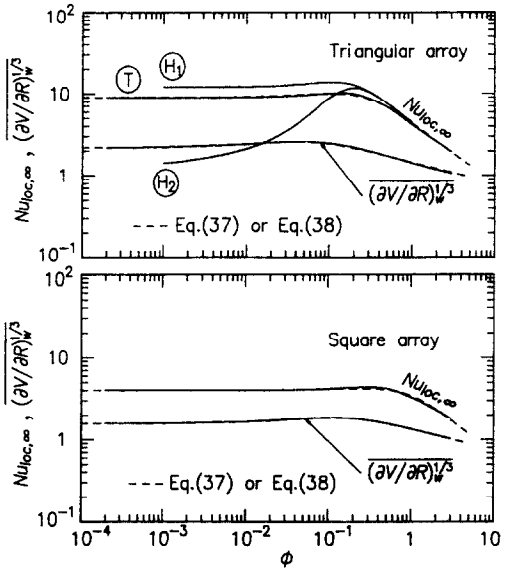

FIG. 5. Variation of asymptotic Nusselt number and mean value of the third root of the velocity gradient at wall with dimensionless spacing between cylinders.

tion shown in Table 3 for a uniform wall temperature both peripherally and axially; (H) represents the solution for a uniform wall temperature peripherally and a uniform wall heat flux axially, and (H2) the solution for a uniform heat flux both peripherally and axially [6]. In each case, $Nu_{\mathrm{loc},\infty}$ increases and then decreases as σ is reduced, while the difference between the values of $Nu_{\mathrm{loc},\infty}$ is reduced, as σ is increased. The variation of $\overline{(\partial V/\partial R)_w^{1/3}}$ in equation (29) with ϕ, which is also shown in Fig. 5, is qualitatively similar to that of $Nu_{\mathrm{loc},\infty}$.

Figures 6 and 7 show the comparison between the numerical results for a triangular array of cylinders and those for a square array of cylinders at the same volume fractions of cylinders ε given by

$$\varepsilon = \frac{\pi r_o^2}{2\sqrt{3}s^2} = \frac{\pi}{2\sqrt{3}\sigma^2}\ [\mathrm{TA}], \quad \varepsilon = \frac{\pi r_o^2}{4s^2} = \frac{\pi}{4\sigma^2}\ [\mathrm{SA}]. \tag{32}$$

Table 3. Asymptotic Nusselt number

	$Nu_{\mathrm{loc},\infty}$, $Nu_{\mathrm{lm},\infty}$	
σ	Triangular array	Square array
1.0	8.92	4.02
1.001	8.93	4.01
1.01	9.02	3.98
1.02	9.13	3.99
1.05	9.52	4.07
1.1	9.97	4.17
1.2	9.89	4.33
1.5	6.86	4.21
2.0	4.17	3.29
4.0	1.96	1.82

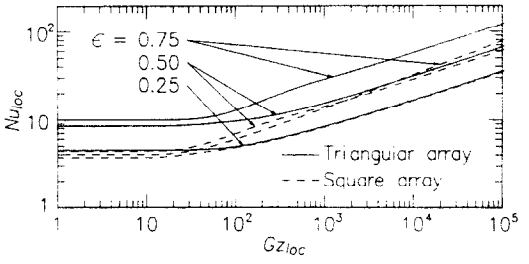

FIG. 6. Comparison of local Nusselt number between triangular and square arrays of cylinders.

As seen from the figures, in general, the heat transfer coefficient for the triangular array is larger than that for the square array, especially for the case $\varepsilon > 0.5$.

6. CORRELATING EQUATIONS FOR THE NUSSELT NUMBER

As shown in Figs. 3 and 4, over the range $\sigma = 1.0$–1.1 [TA] or $\sigma = 1.0$–1.2 [SA], the local and logarithmic-mean Nusselt numbers are only slightly affected by σ and can be expressed as

$$Nu_{\mathrm{loc}} = 9.26(1+0.0022Gz_{\mathrm{loc}}^{1.46})^{1/4} \quad [\mathrm{TA}]$$

$$Nu_{\mathrm{loc}} = 4.08(1+0.0058Gz_{\mathrm{loc}}^{1.46})^{1/4} \quad [\mathrm{SA}] \tag{33}$$

$$Nu_{\mathrm{lm}} = 9.26(1+0.0179Gz^{1.46})^{1/4} \quad [\mathrm{TA}]$$

$$Nu_{\mathrm{lm}} = 4.08(1+0.0349Gz^{1.46})^{1/4} \quad [\mathrm{SA}]. \tag{34}$$

Figure 8 indicates that these two formulas, represented by the solid lines, are quite close to the numerical solutions represented by the keyed symbols, and are therefore satisfactory correlating equations for the Nusselt numbers.

In this connection, for the case $\sigma = 1.0$, that is, for the case of cylinders in contact with one another, Nu_{loc} and Nu_{lm} can be expressed as

$$Nu_{\mathrm{loc}} = 8.92(1+0.0026Gz_{\mathrm{loc}}^{1.46})^{1/4} \quad [\mathrm{TA}]$$

$$Nu_{\mathrm{loc}} = 4.02(1+0.0052Gz_{\mathrm{loc}}^{1.46})^{1/4} \quad [\mathrm{SA}] \tag{35}$$

$$Nu_{\mathrm{lm}} = 8.92(1+0.0143Gz^{1.46})^{1/4} \quad [\mathrm{TA}]$$

$$Nu_{\mathrm{lm}} = 4.02(1+0.0347Gz^{1.46})^{1/4} \quad [\mathrm{SA}]. \tag{36}$$

Over the range $\sigma > 1.1$ [TA] or $\sigma > 1.2$ [SA], the formulas suitable for predicting the Nusselt numbers

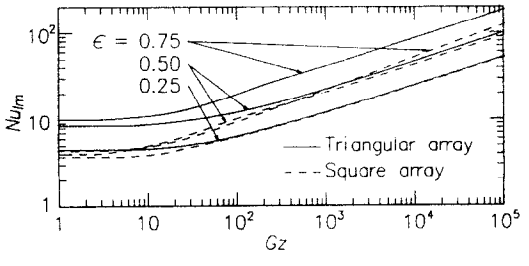

FIG. 7. Comparison of logarithmic-mean Nusselt number between triangular and square arrays of cylinders.

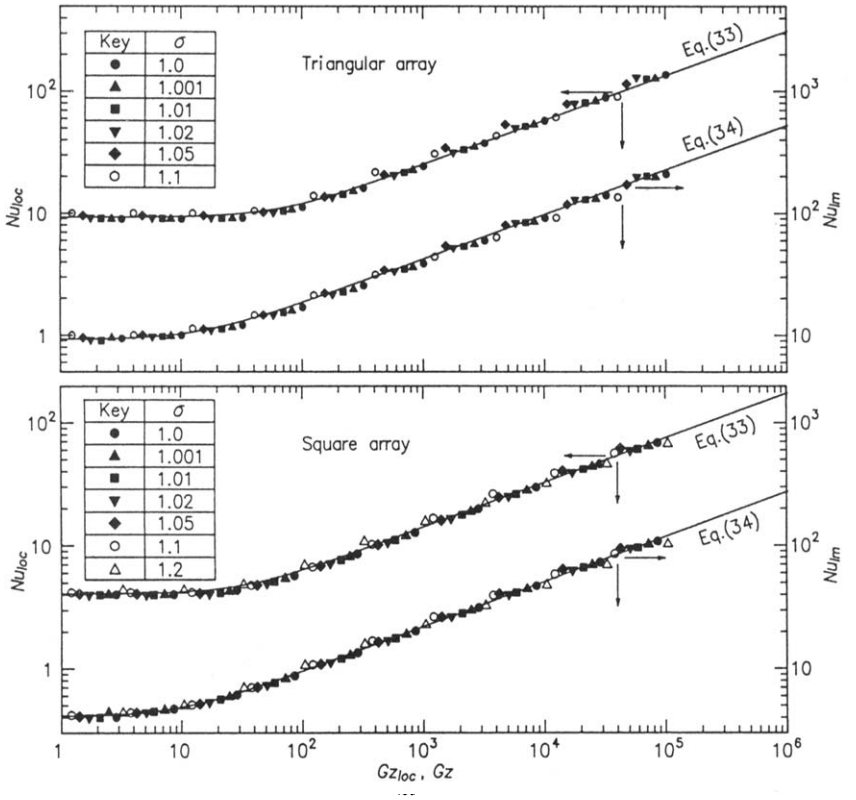

FIG. 8. Comparison of correlating equations (33) and (34) with numerical solutions for small pitch-to-diameter ratios.

can be derived from the asymptotic Nusselt numbers given in Section 3.

The numerical solution shown in Fig. 5 can be formulated as (see broken lines in Fig. 5)

$$Nu_{\mathrm{loc},\infty} = Nu_{\mathrm{lm},\infty} = \frac{8.92(1+2.82\phi)}{(1+6.86\phi^{5/3})} = f \quad \text{[TA]}$$

$$Nu_{\mathrm{loc},\infty} = Nu_{\mathrm{lm},\infty} = \frac{4.00(1+0.509\phi)}{(1+0.765\phi^{5/3})} = f \quad \text{[SA]} \quad (37)$$

$$\overline{(\partial V/\partial R)_w^{1/3}} = \frac{2.17(1+24\phi)}{(1+36.5\phi^{5/4})} \quad \text{[TA]}$$

$$\overline{(\partial V/\partial R)_w^{1/3}} = \frac{1.574(1+9.1\phi)}{(1+10.8\phi^{5/4})} \quad \text{[SA]}. \quad (38)$$

Substituting equation (38) into equation (29) (and setting $\Gamma(4/3) = 0.8930$) gives

$$Nu_{\mathrm{loc},0} = \frac{2.34(1+24\phi)}{(1+36.5\phi^{5/4})(2\sqrt{3}\sigma^2-\pi)^{1/3}} Gz_{\mathrm{loc}}^{1/3} = g\,Gz_{\mathrm{loc}}^{1/3} \quad \text{[TA]}$$

$$Nu_{\mathrm{loc},0} = \frac{1.69(1+9.1\phi)}{(1+10.8\phi^{5/4})(4\sigma^2-\pi)^{1/3}} Gz_{\mathrm{loc}}^{1/3} = g\,Gz_{\mathrm{loc}}^{1/3} \quad \text{[SA]}. \quad (39)$$

Therefore, from equation (31)

$$Nu_{\mathrm{lm},0} = (3/2)g\,Gz^{1/3}. \quad (40)$$

As Gz_{loc} and Gz are increased, the expressions for Nu_{loc} and Nu_{lm} shift from equation (37) to equations (39) and (40), respectively. Hence the expressions of the following form seem reasonable:

$$Nu_{\mathrm{loc}} = (Nu_{\mathrm{loc},\infty}^2 + Nu_{\mathrm{loc},0}^2)^{1/2} \quad (41)$$

$$Nu_{\mathrm{lm}} = (Nu_{\mathrm{lm},\infty}^2 + Nu_{\mathrm{lm},0}^2)^{1/2}. \quad (42)$$

Substituting equations (37), (39) and (40) into equations (41) and (42) gives

$$Nu_{\mathrm{loc}}/f = \{1+(g/f)^2\,Gz_{\mathrm{loc}}^{2/3}\}^{1/2} \quad (43)$$

$$Nu_{\mathrm{lm}}/f = \{1+(3/2)^2(g/f)^2 Gz^{2/3}\}^{1/2}. \quad (44)$$

Figure 9 shows a comparison between equations (43) and (44) (the solid curves) and the numerical solutions (the keyed symbols). The agreement is seen to be reasonably good over the range $\sigma = 1.1$–4.0 [TA] or $\sigma = 1.2$–4.0 [SA], showing that equations (43) and (44) are satisfactory correlating equations for the Nusselt numbers.

7. CONCLUSIONS

A numerical analysis has been carried out to determine the characteristics of laminar-flow heat transfer

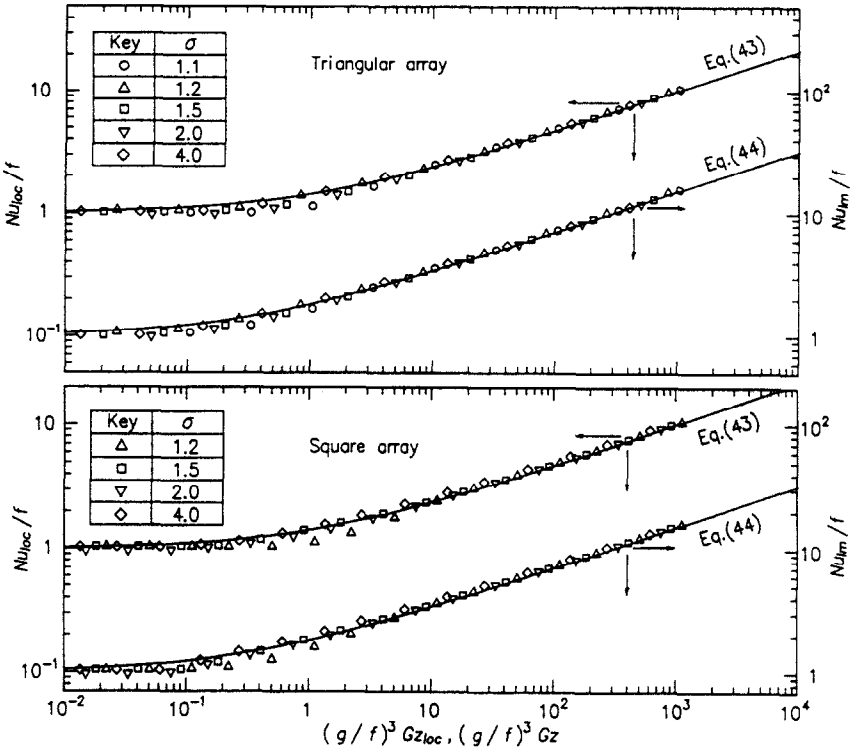

FIG. 9. Comparison of correlating equations (43) and (44) with numerical solutions for large pitch-to-diameter ratios.

to a fluid flowing axially between a triangular array [TA] or a square array [SA] of cylinders with a uniform wall temperature and various pitch-to-diameter ratios σ (or various dimensionless spacings $\phi = \sigma - 1$). The relationships between the local Nusselt number Nu_{loc} and the local Graetz number Gz_{loc}, and between the logarithmic-mean Nusselt number Nu_{lm} and the Graetz number Gz were formulated, for $\sigma = 1.0$–1.1 [TA] or $\sigma = 1.0$–1.2 [SA] as

$$Nu_{loc} = 9.26(1+0.0022Gz_{loc}^{1.46})^{1/4},$$

$$Nu_{lm} = 9.26(1+0.0179Gz^{1.46})^{1/4} \quad \text{[TA]}$$

$$Nu_{loc} = 4.08(1+0.0058Gz_{loc}^{1.46})^{1/4},$$

$$Nu_{lm} = 4.08(1+0.0349Gz^{1.46})^{1/4} \quad \text{[SA]}$$

and, for $\sigma = 1.1$–4.0 [TA] or $\sigma = 1.2$–4.0 [SA] as

$$Nu_{loc} = (f^2 + g^2 Gz_{loc}^{2/3})^{1/2},$$

$$Nu_{lm} = \{f^2 + (3g/2)^2 Gz^{2/3}\}^{1/2}$$

where

$$f = \frac{8.92(1+2.82\phi)}{1+6.86\phi^{5/3}},$$

$$g = \frac{2.34(1+24\phi)}{(1+36.5\phi^{5/4})(2\sqrt{3}\sigma^2-\pi)^{1/3}} \quad \text{[TA]}$$

$$f = \frac{4.00(1+0.509\phi)}{1+0.765\phi^{5/3}},$$

$$g = \frac{1.69(1+9.1\phi)}{(1+10.8\phi^{5/4})(4\sigma^2-\pi)^{1/3}} \quad \text{[SA]}.$$

REFERENCES

1. Am. Soc. Mech. Engng (Editors), *Heat Transfer in Rod Bundles*, ASME (1968).
2. R. K. Shah and A. L. London, *Laminar Flow Forced Convection in Ducts*, Academic Press, New York (1978).
3. E. M. Sparrow, A. L. Loeffler, Jr. and H. A. Hubbard, Heat transfer to longitudinal laminar flow between cylinders, *J. Heat Transfer* **83**, 415 (1961).
4. C.-J. Hsu, Laminar- and slug-flow heat transfer characteristics of fuel rods adjacent to fuel subassembly walls, *Nucl. Sci. Engng* **49**, 398 (1972).
5. V. M. Borishanskii, M. A. Gotovskii and E. V. Firsova, Heat exchange when a liquid metal flows longitudinally through a bundle of rods arranged in a triangular lattice, *Atom. Energiya* **22**, 318 (1967).
6. O. E. Dwyer and H. C. Berry, Laminar-flow heat transfer for in-line flow through unbaffled rod bundles, *Nucl. Sci. Engng* **42**, 81 (1970).
7. K. A. Antonopoulos, Heat transfer in tube assemblies under conditions of laminar axial, transverse and inclined flow, *Int. J. Heat Fluid Flow* **6**, 193 (1985).
8. Y. Abe, Y. Takahashi, R. Sakamoto, K. Kanari, M. Kamimoto and T. Ozawa, Charge and discharge characteristics of a direct contact latent thermal energy storage unit using form-stable high-density polyethylene, *Trans. ASME, J. Sol. Energy Engng* **106**, 465 (1984).
9. E. M. Sparrow and A. L. Loeffler, Jr., Longitudinal

laminar flow between cylinders arranged in regular array, *A.I.Ch.E. Jl* **5**, 325 (1959).
10. J. G. Knudsen and D. L. Katz, *Fluid Dynamics and Heat Transfer*, p. 363. McGraw-Hill, New York (1958).
11. O. Miyatake and H. Iwashita, A numerical analysis of laminar-flow heat transfer to a fluid flowing longitudinally between cylinders with a uniform surface temperature, *Rep. Res. Inst. Ind. Sci., Kyushu Univ.* No. 80, 51 (1986).
12. O. Miyatake, H. Iwashita and N. Miura, A numerical analysis of laminar-flow heat transfer to a fluid flowing axially between a square array of heated cylinders with a uniform surface temperature, *Sogorikogaku Kenkyuka Hokoku, Kyushu Univ.* **9**(2), 69 (1987).

TRANSFERT THERMIQUE POUR UN ECOULEMENT LAMINAIRE DE FLUIDE AXIAL ENTRE DES CYLINDRES A TEMPERATURE DE SURFACE UNIFORME

Résumé—On traite le transfert thermique pour un écoulement laminaire axial de fluide à travers un arrangement triangulaire ou carré de cylindres à température de paroi uniforme. L'équation d'énergie mise sous forme de différences finies est résolue pour obtenir la variation axiale de la distribution de température dans la section droite, et les résultats numériques sont présentés pour le nombre de Nusselt local Nu_{loc} et pour le nombre de Nusselt Nu_{lm} relatif à la moyenne logarithmique. On etablit des formules pour la prédiction de Nu_{loc} et Nu_{lm} en fonction du rapport pas/diamètre σ et du nombre de Graetz local Gz_{loc} et du nombre de Graetz Gz. On trouve que pour une même fraction de volume des cylindres ε, le coefficient de transfert thermique pour l'arrangement triangulaire est supérieur à celui pour l'arrangement carré, spécialement pour le cas $\varepsilon > 0{,}5$.

WÄRMETRANSPORT VON EINEM ROHRBÜNDEL AN EINE LAMINARE LÄNGSANSTRÖMUNG BEI EINHEITLICHER OBERFLÄCHENTEMPERATUR

Zusammenfassung—Der Wärmeübergang in einem laminaren längsdurchströmten Rohrbündel wird untersucht. Die Rohre befinden sich in quadratischer oder in Dreiecksanordnung, die Oberflächentemperatur ist einheitlich. Die Energiebilanz wird in Form von finiten Differenzen gelöst, um die axiale Änderung der Temperaturverteilung in den Strömungsquerschnitten zu bestimmen. Numerische Ergebnisse für die lokale Nusselt-Zahl (Nu_{loc}) und die mittlere logarithmische Nusselt-Zahl (Nu_{lm}) werden ermittelt. Aus den Ergebnissen werden Korrelationsgleichungen zur Berechnung von Nu_{loc} und Nu_{lm} als Funktion des Teilungsverhältnisses (σ) und der lokalen Graetz-Zahl (Gz_{loc}) oder der Graetz-Zahl (Gz) angegeben. Es zeigt sich, daß—bei einem konstanten Volumenanteil (ε) der Zylinder—der Wärmeübergangskoeffizient für eine Dreiecksanordnung größer ist als bei einer quadratischen Anordnung. Dies gilt insbesondere für den Fall $\varepsilon > 0{,}5$.

ТЕПЛОПЕРЕНОС ОТ ЛАМИНАРНОГО ПОТОКА К АКСИАЛЬНОМУ ОТОКУ ЖИДКОСТИ МЕЖДУ ЦИЛИНДРАМИ С ОДИНАКОВОЙ ТЕМПЕРАТУРОЙ ПОВЕРХНОСТИ

Аннотация—Исследуется теплоперенос от ламинарного потока к аксиальному потоку жидкости между цилиндрами с одинаковой температурой стенок, расположенными в шахматном или коридорном порядке. Уравнение сохранения энергии решается конечно-разностным методом для определения аксиального изменения распределения температуры в поперечном сечении. Представлены численные результаты для локального Nu_{loc} и логарифмического среднего Nu_{lm} чисел Нуссельта. На основе полученных результатов выводятся корреляционные соотношения для расчета Nu_{loc} и Nu_{lm} в зависимости от отношения шага к диаметру σ и от локального числа Гретца Gz_{loc} или числа Гретца Gz. Найдено, что при одинаковых объемных долях цилиндров ε коэффициент теплопереноса в случае шахматного расположения цилиндров больше, чем в случае коридорного, особенно когда $\varepsilon > 0{,}5$.